IEEE Access
Multidisciplinary | Rapid Review | Open Access Journal

Received September 13, 2018, accepted October 1, 2018, date of publication October 18, 2018, date of current version November 9, 2018.

Digital Object Identifier 10.1109/ACCESS.2018.2876323

Position Determination for Moving Transmitter Using Single Station

YIMAO SUN[1,2], (Student Member, IEEE), AND QUN WAN[1], (Member, IEEE)
[1]School of Information and Communication Engineering, University of Electronic Science and Technology of China, Chengdu 611731, China
[2]Electrical Engineering and Computer Science Department, University of Missouri, Columbia, MO 65211, USA

Corresponding author: Qun Wan (wanqun@uestc.edu.cn)

This work was supported in part by the National Natural Science Foundation of China under Grant U1533125, Grant 61471153, and Grant 61771108, in part by the National Science and Technology Major Project under Grant 2016ZX03001022, in part by the Fundamental Research Funds for the Central Universities under Grant ZYGX2015Z011, and in part by the China Scholarship Council.

ABSTRACT A common case in location problem is that the terminal is unstable or moving. The classical methods construct equations related to the measurements observed at the individual receivers first, and then solves the problem to localize the source. In this paper, we focus on the moving transmitter localization problem using only one station. The thinking of inverse synthesis aperture is implied, which takes advantage of the motion model to increase the equivalent aperture for higher accuracy. The proposed method formulates the problem through the angle of arrival and Doppler frequency measurements that are obtained from independent observations. After pseudo linearization by ignoring higher order noise terms, the estimator of position and velocity is easily solved through weighted least squares method. The bias reduction (BR) is utilized for lower bias and better root-mean-square error (RMSE). Using the result of BR as an initial solution, the maximum likelihood estimator (MLE) is realized through Gauss–Newton iteration. Theoretical analysis verifies that the BR estimator is efficient, which has Cramér-Rao Lower Bound (CRLB) accuracy if the noise level is mild. While MLE attends CRLB in higher noise situation albeit the possible divergence problem. Simulations indicate the feasibility and validate the advocated performance. The RMSE and bias match the theory very well.

INDEX TERMS Moving transmitter localization, single station, AOA, Doppler, bias reduction, maximum likelihood estimator.

I. INTRODUCTION

An important problem in communication, navigation, seismology and internet of things is determining the location of radiating source by passive receivers [1]. In the past few decades, this problem has been extensively studied and many methods have been proposed [2], [3].

Classical localization methods utilize intermediate parameters estimated from the received signals to determine the location, e. g., time of arrival (TOA) [4], angle of arrival (AOA) [5], time difference of arrival (TDOA) [6]–[8], and Doppler shift or frequency difference of arrival (FDOA) [9]–[12] for relative moving source and receivers. So they are called two-step methods in some literature [13], [14]. For improving the location accuracy of these methods, a series of hybrid schemes are proposed [15]–[17]. It is introduced in [15] that a simple closed-form method for the 3D point source with TDOA and AOAs has been proposed, which can attain the Cramér-Rao Lower Bound (CRLB) under Gaussian noise. Reference [16] implies this weighted least square (WLS) method to TOA and AOAs case which combined a passive and an active stations.

For decades of years, the moving target localization has been well studied. An algebraic solution for the position and velocity of a moving source using the TDOAs and FDOAs is proposed in [9]. In the presence of random errors in receiver locations, reference [10] performs analysis and develops a solution for locating a moving source using TDOA and FDOA measurements. Exploiting the multidimensional scaling (MDS) analysis, [18] presents an accurate and closed-form solution for the position and velocity of a moving target through TDOA and FDOA measurements collected by an array of passive sensors. Reference [12] resorts to semidefinite relaxation (SDR) to convert the optimization problem to convex semidefinite programming then solving by CVX[1] directly. Reference [11] handles the constrained weighted least squares (CWLS) problem that is established through

[1]CVX is a Matlab-based modeling system for convex optimization (http://cvxr.com/cvx/).

TDOA and FDOA measurements by Newton's method. It results CRLB performance even a sufficiently high noise level before the thresholding effect occurs. In the passive radar system, a two-stage weighted least squares (2WLS) based method is developed using time delay and Doppler shift in [19], which achieves the CRLB in theory.

However, the methods above are for multiple receivers system. The researches on localizing a moving source by single receiver are less studied. It is the first time that a Direct Position Determination (DPD) method for multiple transmitters based on the single moving array has been proposed in [20]. But that paper, including others exploiting Doppler information [13], [21], only considers the motion of receivers where the transmitters are stationary. Moving receivers not only obtain additional measurements such as Doppler frequency, but also increase the equivalent aperture of an antenna. This has been validated in Synthesis Aperture Radar (SAR) [22]–[24]. Similarly, Inverse Synthesis Aperture Radar (ISAR) achieves a similar purpose while surveilling moving targets using fixed receiver [25]. We could extend this thinking exploited in ISAR imaging to localization problem to estimate the position and track a moving target. Indeed, to the best of our knowledge, we have not come across a maximum likelihood estimator (MLE) that is to handle a single station localization scenario.

This paper focuses on the moving transmitter localization problem based on single station. We imply the thinking of ISA to localization and develop several single station localization methods for moving transmitter. The proposed algorithms estimate the initial position and velocity through AOA and Doppler frequency measurements obtained from independent observations. We validate that weighted total least squares (WTLS) has poor accuracy in even moderate signal-to-noise ratio (SNR) first. Then an improved bias reduction (BR) method that reduces the bias efficiently is derived. Using the BR solution as the initial value, the associated MLE is realized through Gauss-Newton iteration. Theoretical analysis in details in terms of the mean-square error (MSE) and bias are provided subsequently. The MSE analytical results illustrate that both BR and MLE are able to attain the CRLB performance in position and velocity at a mild noise level with appropriate snapshots and observations. The theoretical bias predicts the solution performance well. The initial solution is analytic-form. And the iteration of MLE will converge rapidly if the initial value is close to the true value. It is less computation complexity and time consumption than grid searching method such as DPD.

The rest of this paper is organized as follow: Section II formulates the signal model and the problem. The WTLS solution is discussed in the first subsection of Section III to show its limitation. The improvement of bias reduction and MLE are proposed in the next two subsections. Section IV analyzes the theoretical performance via MSE and bias. Then the analytical MSE results are compared with CRLB. Simulations are outlined in Section VI and Section VII concludes this paper.

TABLE 1. Notations.

Symbol	Description
$\mathbf{a}$, $\mathbf{A}$	vector and matrix
$\{*\}^T$, $\{*\}^H$	transpose and conjugate transpose
$a(i)$	the i-th element of $\mathbf{a}$
$\mathbf{a}(i:j)$	subvector formed by the i-th to the j-th element
$\|\mathbf{a}\|$	Euclidean norm of $\mathbf{a}$
$\mathbf{A}(i,:)$ and $\mathbf{A}(:,j)$	the i-th row and the j-th column of $\mathbf{A}$
$\mathrm{diag}\{\mathbf{a}\}$	diagonal matrix with the elements of $\mathbf{a}$ as the diagonal
$\mathrm{blkdiag}\{(*),\cdots,(\bullet)\}$	block diagonal matrix with diagonal blocks $(*),\cdots,(\bullet)$
$\mathbf{I}_N$	identity matrix of size $N\times N$
$\mathbf{O}_{M\times N}$	all-zero matrix of size $M\times N$
$\mathbf{1}_N$, $\mathbf{0}_N$	column vectors of 1 or 0 of length N
$\mathbf{a}^o$	true value of a noisy quantity $\mathbf{a}$
$\Delta\mathbf{a}$	difference of $\mathbf{a}$ and its true value
$\arctan(a/b)$	arc-tangent operation applied to a/b with the quadrant taken into account
$\Re\{*\}$, $\Im\{*\}$	real and imagery parts
$\mathrm{tr}(*)$	trace of matrix

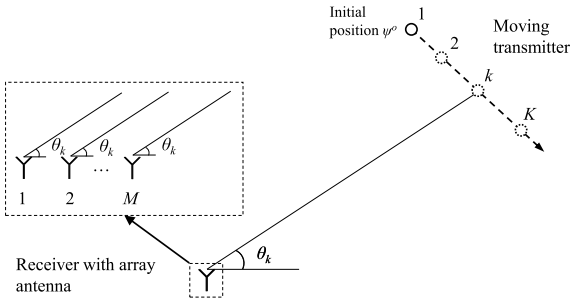

FIGURE 1. Localization scenario.

Following the convention, this paper uses unified symbols and notations defined in Table 1.

II. PROBLEM FORMULATION

Consider a narrow band signal transmitter moving from the initial position $\mathbf{p}^o = [x^o, y^o]^T$ with velocity $\mathbf{v}^o = [v_x^o, v_y^o]^T$. The signal is observed by a stationary station located at $\mathbf{q} = [x_s, y_s]^T$, which equips an array with M elements. And the element spacing is not more than half the wavelength. The source range is far enough so that plane-wave assumption is satisfied. The observing time T_s is short enough so that position and velocity can be assumed temporarily stationary during the observing. The scenario is shown in Fig. 1.

Denote vector $\boldsymbol{\psi}^o = [\mathbf{p}^{oT}, \mathbf{v}^{oT}]^T$. The k-th interrupted signal started at time t_k after down conversion the frequency is, with known carrier wave,

$$\mathbf{r}_k(t) = b_k\mathbf{a}_k(\boldsymbol{\psi}^o)s_k(t)e^{j2\pi f_k(\boldsymbol{\psi}^o)t} + \boldsymbol{\eta}_k(t) \in \mathbb{C}^{M\times 1}, \quad (1)$$

where $t \in [0, T_s]$, $T_s \ll t_k$. b_k is an unknown complex scalar representing the signal attenuation due to path loss. $\mathbf{a}_k(\boldsymbol{\psi}^o)$

is array response to the k-th frame signal transmitted from $\mathbf{p}$. $s_k(t)$ is a complex signal with known waveform. And $f_k(\boldsymbol{\psi}^o)$ is Doppler frequency

$$f_k(\boldsymbol{\psi}^o) = -\frac{1}{\lambda}\frac{\mathbf{v}^T(\mathbf{p}_k^o - \mathbf{q})}{\|\mathbf{p}_k^o - \mathbf{q}\|}, \tag{2}$$

where

$$\mathbf{p}_k^o = [x_k^o, y_k^o]^T \tag{3}$$

represents the position while the k-th observation. λ is the wavelength of the carrier. The vector $\boldsymbol{\eta}_k(t)$ represents the complex Gaussian noise with zero-mean including multipath and interference, which is assumed independent across transmit bands, time, and array elements. $k = 1, 2, \cdots, K$, and K is the total observation number.

For a linear array, $\mathbf{a}_k(\boldsymbol{\psi}^o)$ could be represented as

$$\mathbf{a}_k(\boldsymbol{\psi}^o) = \begin{bmatrix} e^{j2\pi d_1 \cos\theta_k(\boldsymbol{\psi}^o)/\lambda} \\ e^{j2\pi d_2 \cos\theta_k(\boldsymbol{\psi}^o)/\lambda} \\ \cdots \\ e^{j2\pi d_M \cos\theta_k(\boldsymbol{\psi}^o)/\lambda} \end{bmatrix} \tag{4}$$

where $d_1, \cdots, d_M$ are the distances between the reference element and others. Without losing of generality, we chose the first element as the reference, where $d_1 = 0$. $\theta_k(\boldsymbol{\psi}^o)$ is the k-th direction of arrival

$$\theta_k(\boldsymbol{\psi}^o) = \arctan\frac{y_k^o - y_s}{x_k^o - x_s}. \tag{5}$$

The received signal (1) is sampled by a sequence $t_n = n/f_s$, $n = 0, 1, \cdots, N-1$,

$$\mathbf{r}_k(n) = b_k\bar{\mathbf{a}}_k(n, \boldsymbol{\psi}^o)s_k(n) + \boldsymbol{\eta}_k(n), \tag{6}$$

where

$$\bar{\mathbf{a}}_k(n, \boldsymbol{\psi}^o) = \mathbf{a}_k(\boldsymbol{\psi}^o)\epsilon_k(n, \boldsymbol{\psi}^o), \tag{7a}$$
$$\epsilon_k(n, \boldsymbol{\psi}^o) = e^{j2\pi f_k(\boldsymbol{\psi}^o)n/f_s}, \tag{7b}$$

f_s is sample frequency. Stacking the snapshots in a vector form gives

$$\mathbf{r}_k = b_k\mathbf{A}_k\mathbf{s}_k + \boldsymbol{\eta}_k \in \mathbb{C}^{MN\times 1}, \tag{8}$$

where

$$\mathbf{r}_k = \left[\mathbf{r}_k^T(0), \mathbf{r}_k^T(1)\cdots\mathbf{r}_k^T(N-1)\right]^T, \tag{9a}$$
$$\mathbf{A}_k = \text{blkdiag}\{\bar{\mathbf{a}}_k(0, \boldsymbol{\psi}), \ldots, \bar{\mathbf{a}}_k(N-1, \boldsymbol{\psi})\}, \tag{9b}$$
$$\mathbf{s}_k = [s_k(0), s_k(1), \cdots, s_k(N-1)]^T, \tag{9c}$$
$$\boldsymbol{\eta}_k = [\boldsymbol{\eta}_k^T(0), \boldsymbol{\eta}_k^T(1), \cdots, \boldsymbol{\eta}_k^T(N-1)]^T. \tag{9d}$$

Equation (8) is called a frame which includes N samples.

We are interested in estimating the source initial location using the received signals. Tracking is direct according the motion model.

III. THE PROPOSED METHOD

Traditional location methods usually estimate the intermediate parameters first, then localize the source using these results. In this problem, we can measurement the AOA and Doppler first in terms of the received signal (1). Plenty of researches have been developed on AOA [26]–[29] and Doppler [30]–[32] estimating. We can get the required parameters for localization through these methods. To limit our scope, the rest of this section only discusses how to use these intermediate parameters to estimate the position and velocity. For simplicity, it is assumed that the interested source is constant speed [33].

Denoting the estimation of AOA and Doppler $\boldsymbol{\gamma} = [\boldsymbol{\theta}^T, \mathbf{f}^T]^T$ is zero-mean with covariance matrix $\mathbf{Q} = \text{blkdiag}\{[\mathbf{Q}_a, \mathbf{Q}_f]\}$, where $\mathbf{Q}_a$ and $\mathbf{Q}_f$ are the covariance matrices of AOAs $\boldsymbol{\theta} = [\theta_1, \cdots, \theta_K]^T$ and Dopplers $\mathbf{f} = [f_1, \cdots, f_K]^T$ respectively. f_k and θ_k are defined in (2) and (5), where $(\boldsymbol{\psi})$ has been neglected. The AOA and Doppler are assumed independent. Taking tangent on the both sides of (5), after simplifying yields

$$\mathbf{u}_k^{oT}\mathbf{p}_k^o = \mathbf{u}_k^{oT}\mathbf{q}. \tag{10}$$

Under the constant speed assumption, we have

$$\mathbf{p}_k^o = \mathbf{p}^o + t_k\mathbf{v}^o. \tag{11}$$

Applying (11) to (10),

$$\mathbf{u}_k^{oT}\mathbf{p}^o + t_k\mathbf{u}_k^{oT}\mathbf{v}^o = \mathbf{u}_k^{oT}\mathbf{q}, \tag{12}$$

where $\mathbf{u}_k^o$ is unit vector given by

$$\mathbf{u}_k^o = [\sin\theta_k^o, -\cos\theta_k^o]^T. \tag{13}$$

Define

$$\bar{\mathbf{p}}_k^o = \frac{\mathbf{p}_k^o - \mathbf{q}}{\|\mathbf{p}_k^o - \mathbf{q}\|}, \tag{14}$$

equation (2) can be written as

$$\lambda f_k^o + \bar{\mathbf{p}}_k^{oT}\mathbf{v}^o = 0. \tag{15}$$

In the presence of noise, the measurements can be expressed as their true value adding the noise,

$$\boldsymbol{\gamma} = \boldsymbol{\gamma}^o + \Delta\boldsymbol{\gamma}, \tag{16}$$

where

$$\begin{aligned} \Delta\boldsymbol{\gamma} &= [\Delta\boldsymbol{\theta}^T, \Delta\mathbf{f}^T]^T, \\ \Delta\boldsymbol{\theta} &= [\Delta\theta_1, \cdots, \Delta\theta_K]^T, \\ \Delta\mathbf{f} &= [\Delta f_1, \cdots, \Delta f_K]^T. \end{aligned} \tag{17}$$

Applying

$$\begin{aligned} \sin\theta_k &\simeq \sin\theta_k^o + \cos\theta_k^o\Delta\theta_k, \\ \cos\theta_k &\simeq \cos\theta_k^o - \sin\theta_k^o\Delta\theta_k, \end{aligned} \tag{18}$$

to (13) and (14) results

$$\begin{aligned} \mathbf{u}_k^o &= \mathbf{u}_k - \Delta\mathbf{u}_k \\ \Delta\mathbf{u}_k &\simeq [\cos\theta_k^o, \sin\theta_k^o]^T\Delta\theta_k \end{aligned}$$

$$= \bar{\mathbf{p}}_k^o \Delta\theta_k \tag{19}$$

and

$$\begin{aligned} \bar{\mathbf{p}}_k^o &= \bar{\mathbf{p}}_k - \Delta\bar{\mathbf{p}}_k \\ \Delta\bar{\mathbf{p}}_k &\simeq [-\sin\theta_k^o, \cos\theta_k^o]^T \Delta\theta_k \\ &= -\mathbf{u}_k^o \Delta\theta_k. \end{aligned} \tag{20}$$

Substituting (19) and (20) to (10) and (15) reaches

$$\mathbf{u}_k^T \mathbf{q} - (\mathbf{u}_k^T \mathbf{p}^o + t_k \mathbf{u}_k^T \mathbf{v}^o) = b_k \Delta\theta_k, \tag{21a}$$

$$\lambda f_k + \bar{\mathbf{p}}_k^T \mathbf{v}^o = c_k \Delta\theta_k^o + \lambda \Delta f_k, \tag{21b}$$

where

$$\begin{aligned} b_k &= \bar{\mathbf{p}}_k^{oT}(\mathbf{q} - \mathbf{p}^o - t_k \mathbf{v}^o), \\ c_k &= -\mathbf{u}_k^{oT} \mathbf{v}^o. \end{aligned} \tag{22}$$

Stacking (21a) and (21b) together across all K measurements yields

$$\mathbf{h} - \mathbf{G}\boldsymbol{\psi}^o = \mathbf{B}\Delta\boldsymbol{\gamma}. \tag{23}$$

The vector $\mathbf{h}$ and matrices $\mathbf{G}$, $\mathbf{B}$ are

$$\mathbf{h} = [\mathbf{h}_1^T, \mathbf{h}_2^T]^T, \tag{24}$$

where

$$\mathbf{h}_1 = [\mathbf{u}_1, \cdots, \mathbf{u}_K]^T \mathbf{q}, \tag{25a}$$

$$\mathbf{h}_2 = \lambda \mathbf{f}, \tag{25b}$$

and

$$\mathbf{G} = [\mathbf{G}_1^T, \mathbf{G}_2^T]^T, \tag{26}$$

where

$$\mathbf{G}_1 = \begin{bmatrix} \mathbf{u}_1^T & t_1 \mathbf{u}_1^T \\ \vdots & \vdots \\ \mathbf{u}_K^T & t_K \mathbf{u}_K^T \end{bmatrix}, \tag{27a}$$

$$\mathbf{G}_2 = \begin{bmatrix} \mathbf{0}^T & -\bar{\mathbf{p}}_1^T \\ \vdots & \vdots \\ \mathbf{0}^T & -\bar{\mathbf{p}}_K^T \end{bmatrix}, \tag{27b}$$

and

$$\mathbf{B} = \begin{bmatrix} \mathbf{B}_1 & \mathbf{O} \\ \mathbf{B}_2 & \mathbf{B}_3 \end{bmatrix}, \tag{28}$$

where

$$\mathbf{B}_1 = \mathrm{diag}\{[b_1, \cdots, b_K]\}, \tag{29a}$$

$$\mathbf{B}_2 = \mathrm{diag}\{[c_1, \cdots, c_K]\}, \tag{29b}$$

$$\mathbf{B}_3 = \lambda \mathbf{I}. \tag{29c}$$

The unknown $\boldsymbol{\psi}^o$ is linear in the equation error expression (23) and we can apply the least-squares criterion to obtain the solution. In order to balance the errors from different rows of (23), the weighting matrix is introduced, leading to the weighted least-squares minimization criterion. Thus, finding $\boldsymbol{\psi}^o$ is solving the quadratic optimization problem

$$\min_{\boldsymbol{\psi}} (\mathbf{h} - \mathbf{G}\boldsymbol{\psi})^T \mathbf{W} (\mathbf{h} - \mathbf{G}\boldsymbol{\psi}), \tag{30}$$

where

$$\mathbf{W} = E[\mathbf{B}\Delta\boldsymbol{\gamma}\Delta\boldsymbol{\gamma}^T\mathbf{B}^T]^{-1} \simeq \mathbf{B}^{-1}\mathbf{Q}^{-1}\mathbf{B}^{-T} \tag{31}$$

is the weighting matrix.

A. WTLS BASED SOLUTION

Equation (30) is a WLS problem. However, $\mathbf{G}$ is ill-posed since the near-linearity between its columns, solving (30) by WLS will result to unreliable performance. We resort to weighted total least squares (WTLS), which has the ability to restrain the perturbation of $\mathbf{G}$, to minimize the noise of both $\mathbf{G}$ and $\mathbf{h}$. Constructing an augmented matrix

$$\widetilde{\mathbf{G}} = [-\mathbf{G}, \mathbf{h}], \tag{32}$$

the problem in (30) becomes

$$\min_{\widetilde{\boldsymbol{\psi}}} \widetilde{\boldsymbol{\psi}}^T \widetilde{\mathbf{G}}^T \mathbf{W} \widetilde{\mathbf{G}} \widetilde{\boldsymbol{\psi}}, \tag{33}$$

where $\widetilde{\boldsymbol{\psi}}^o = [\boldsymbol{\psi}^{oT}, 1]^T$. Solving (33) by singular value decomposition (SVD) of $\widetilde{\mathbf{G}}^T\mathbf{W}\widetilde{\mathbf{G}}$,

$$\mathbf{U}\boldsymbol{\Lambda}\mathbf{V}^T = \widetilde{\mathbf{G}}^T \mathbf{W} \widetilde{\mathbf{G}}, \tag{34}$$

where $\boldsymbol{\Lambda}$ is a diagonal matrix constructed by the singular value of $\widetilde{\mathbf{G}}^T\mathbf{W}\widetilde{\mathbf{G}}$. Let $\boldsymbol{\nu}$ be the right singular vector corresponding to the minimum singular value. The estimator of position and velocity is given by

$$\boldsymbol{\psi} = \boldsymbol{\nu}(1:4)/\nu(5). \tag{35}$$

The weighting matrix in (34) depends on the true position and velocity that are not known in practice. To handle this problem, we can instead (31) by $\mathbf{Q}^{-1}$ to obtain an initial estimate for the source position and velocity. For implementation purpose, it is reasonable to replace the true AOA and Doppler values in $\mathbf{B}$ by their measurements. Then applying the initial estimate, together with the angle and Doppler measurements, the weighting matrix can be computed via (22), (28) and (31). Updating $\mathbf{W}$ one or two times is sufficient.

B. BIAS REDUCTION

Usually the WTLS restraining the perturbation is able to reduce bias. However, it is not sufficient to handle our problem. Simulation results (Fig. 2 and Fig. 3) show that WTLS has the thresholding effect when SNR is lower than 6 dB due to the bias increases rapidly, which dominants the root-mean-square error (RMSE). Therefore, it is necessary to find a solution reducing the bias further. It should be noted that the bias reduction method is proposed for TDOA location problem for the first time in [34]. Following the idea reaches our solution.

Noting that $\widetilde{\mathbf{G}}$ contains measurement noise, it is decomposed as

$$\widetilde{\mathbf{G}} = \widetilde{\mathbf{G}}^o + \Delta\widetilde{\mathbf{G}}, \tag{36}$$

where

$$\Delta\widetilde{\mathbf{G}} = [-\Delta\mathbf{G}, \Delta\mathbf{h}], \tag{37}$$

$\Delta\mathbf{G}$ and $\Delta\mathbf{h}$ are defined by (91)-(94). Then putting (36) to the cost function in the optimization problem (33), a transformed form is obtained,

$$\mathcal{J}_{WTLS} = \widetilde{\boldsymbol{\psi}}^T\widetilde{\mathbf{G}}^{oT}\mathbf{W}\widetilde{\mathbf{G}}^o\widetilde{\boldsymbol{\psi}} + \widetilde{\boldsymbol{\psi}}^T\Delta\widetilde{\mathbf{G}}^T\mathbf{W}\Delta\widetilde{\mathbf{G}}\widetilde{\boldsymbol{\psi}} + 2\widetilde{\boldsymbol{\psi}}^T\widetilde{\mathbf{G}}^{oT}\mathbf{W}\Delta\widetilde{\mathbf{G}}\widetilde{\boldsymbol{\psi}}. \quad (38)$$

Equation (38) shows that the noise term $\Delta\widetilde{\mathbf{G}}$ perturbs the cost function we minimized, which results the large bias in solutions. Since $\Delta\boldsymbol{\theta}$ and $\Delta\mathbf{f}$ are assumed zero-mean, the expectation of the last term is zero. Taking expectation of (38), we obtain

$$\mathcal{J}_{BR} = \widetilde{\boldsymbol{\psi}}^T\widetilde{\mathbf{G}}^{oT}\mathbf{W}\widetilde{\mathbf{G}}^o\widetilde{\boldsymbol{\psi}} + \widetilde{\boldsymbol{\psi}}^T E[\Delta\widetilde{\mathbf{G}}^T\mathbf{W}\Delta\widetilde{\mathbf{G}}]\widetilde{\boldsymbol{\psi}}. \quad (39)$$

To eliminate the perturbation by the second term of (39), we shall constrain it constant. Therefore, the problem (33) is transformed to find $\widetilde{\boldsymbol{\psi}}$ through

$$\min_{\widetilde{\boldsymbol{\psi}}} \widetilde{\boldsymbol{\psi}}^T\widetilde{\mathbf{G}}^T\mathbf{W}\widetilde{\mathbf{G}}\widetilde{\boldsymbol{\psi}} \quad \text{s.t. } \widetilde{\boldsymbol{\psi}}^T\boldsymbol{\Omega}\widetilde{\boldsymbol{\psi}} = const., \quad (40)$$

where

$$\boldsymbol{\Omega} = E[\Delta\widetilde{\mathbf{G}}^T\mathbf{W}\Delta\widetilde{\mathbf{G}}]. \quad (41)$$

The expression of $\boldsymbol{\Omega}$ is detailed in Appendix A.

Constructing the Lagrangian and differentiating it, then setting the result to zero yield

$$\widetilde{\mathbf{G}}^T\mathbf{W}\widetilde{\mathbf{G}}\widetilde{\boldsymbol{\psi}} = \xi\boldsymbol{\Omega}\widetilde{\boldsymbol{\psi}}, \quad (42)$$

where ξ is the Lagrange multiplier. Hence the solution is the generalized eigenvector of the pair $\{\widetilde{\mathbf{G}}^T\mathbf{W}\widetilde{\mathbf{G}}, \boldsymbol{\Omega}\}$ that minimize the cost function defined in (33).

Dividing the first 4 elements by the last, the final solution is

$$\boldsymbol{\psi} = \widetilde{\boldsymbol{\psi}}(1:4)/\widetilde{\psi}(5). \quad (43)$$

The weighting matrix $\mathbf{W}$ can be set as $\mathbf{Q}^{-1}$ instead of (31) to obtain an initial estimate. Then applying this result, together with the measurements, $\mathbf{W}$ can be updated via (22), (28) and (31). Iterating one or two times is sufficient. The rest problem is that $\mathbf{P}_1$, $\mathbf{P}_2$ and $\mathbf{P}_3$ rely on the true AOA. Replacing the true angle by the measurements and the lost in performance is negligible.

C. MLE

The theoretical covariance analyzed in Section IV-B.1 is proved matching the CRLB in Appendix B. Nevertheless, it requires sufficient SNR or small noise. The MLE is proposed to improve the performance in low SNR case. We apply the result supplied by Subsection III-B as the initial value to get the MLE. The estimator is the minimizer of the cost function

$$\mathcal{J}_{ML} = (\boldsymbol{\gamma} - \bar{\boldsymbol{\gamma}}(\boldsymbol{\psi}))^T\mathbf{Q}^{-1}(\boldsymbol{\gamma} - \bar{\boldsymbol{\gamma}}(\boldsymbol{\psi})), \quad (44)$$

where $\bar{\boldsymbol{\gamma}}(\boldsymbol{\psi})$ is the reconstructed measurements according to (2) and (5) by replacing the true position and velocity with the optimization variable $\boldsymbol{\gamma}$. A common approach for solving this problem is through iteration using the Gauss-Newton method.

Denoting $\boldsymbol{\psi}^{(0)}$ is the initial solution, taking Taylor-series expansion of $\bar{\boldsymbol{\gamma}}(\boldsymbol{\psi})$ at $\boldsymbol{\psi}^{(0)}$ and keeping up the first order terms give a quadratic approximation of $\mathcal{J}_{ML}$. Differentiating it with respect to $\boldsymbol{\psi}$ and setting the result to zero yield the Gauss-Newton iterative equation for solving the unknown,

$$\boldsymbol{\psi}^{(i+1)} = \boldsymbol{\psi}^{(i)} + (\mathbf{K}^{(i)T}\mathbf{Q}^{-1}\mathbf{K}^{(i)})^T\mathbf{K}^{(i)T}\mathbf{Q}^{-1}(\boldsymbol{\gamma} - \bar{\boldsymbol{\gamma}}(\boldsymbol{\psi}^{(i)})), \quad (45)$$

where $i = 1, 2, \cdots$, and

$$\mathbf{K}^i = \left.\frac{\partial\bar{\boldsymbol{\gamma}}(\boldsymbol{\psi})}{\partial\boldsymbol{\psi}^T}\right|_{\boldsymbol{\psi}=\boldsymbol{\psi}^{(i)}}. \quad (46)$$

The expression of $\mathbf{K}^i$ is given by (49)-(51) replacing the true value with the iterated $\boldsymbol{\psi}^{(i)}$.

IV. PERFORMANCE ANALYSIS

In this section, we shall provide the CRLB for both position and velocity, which investigates the performance of the estimators from those methods. The covariance analysis is first order where the higher order noise term are ignored and it is valid over the small error region only. The bias evaluation is up to the second order noise terms.

A. CRLB

We start from angle and Doppler measurements for the proposed, where their estimation performance is discussed in Appendix C.

The CRLB is given by [35]

$$\mathbf{CRLB}(\boldsymbol{\psi}^o) = \mathbf{FIM}^{-1}(\boldsymbol{\psi}^o), \quad (47)$$

where $\mathbf{FIM}(\boldsymbol{\psi}^o)$ is Fisher Information Matrix (FIM),

$$\mathbf{FIM}(\boldsymbol{\psi}^o) = \frac{\partial\boldsymbol{\gamma}^{oT}}{\partial\boldsymbol{\psi}^o}\mathbf{Q}^{-1}\frac{\partial\boldsymbol{\gamma}^o}{\partial\boldsymbol{\psi}^{oT}}. \quad (48)$$

The expression of the partial derivative of $\boldsymbol{\gamma}^o$ with respect to $\boldsymbol{\psi}^o$ is

$$\frac{\partial\boldsymbol{\gamma}^o}{\partial\boldsymbol{\psi}^{oT}} = \left[\frac{\partial\theta_1^o}{\partial\boldsymbol{\psi}^o}, \cdots, \frac{\partial\theta_K^o}{\partial\boldsymbol{\psi}^o}, \frac{\partial f_1^o}{\partial\boldsymbol{\psi}^o}, \cdots, \frac{\partial f_k}{\partial\boldsymbol{\psi}^o}\right]^T, \quad (49)$$

where

$$\frac{\partial\theta_k^o}{\partial\boldsymbol{\psi}^o} = \frac{1}{r_k^{o2}}\begin{bmatrix} -(y_k^o - y_s) \\ x_k^o - x_s \\ -t_k(y_k^o - y_s) \\ t_k(x_k^o - x_s)\end{bmatrix}, \quad (50)$$

and

$$\frac{\partial f_k^o}{\partial\boldsymbol{\psi}^o} = \left[\frac{\partial f_k^o}{\partial\mathbf{p}^{oT}}, \frac{\partial f_k^o}{\partial\mathbf{v}^{oT}}\right]^T, \quad (51)$$

where

$$\frac{\partial f_k^o}{\partial\mathbf{p}^o} = \frac{\mathbf{v}^o}{r_k^o} - \frac{(\mathbf{p}_k^o - \mathbf{q})^T\mathbf{v}^o(\mathbf{p}_k^o - \mathbf{q})}{r_k^{o3}},$$

$$\frac{\partial f_k^o}{\partial \mathbf{v}^o} = \frac{(\mathbf{p}_k^o - \mathbf{q}) + t_k \mathbf{v}^o}{r_k^o} - \frac{t_k (\mathbf{p}_k^o - \mathbf{q}) \mathbf{v}^o (\mathbf{p}_k^o - \mathbf{q})}{r_k^{o3}}. \quad (52)$$

The r_k^o in (50) and (52) is $\|\mathbf{p}_k^o - \mathbf{q}\|$.

B. COVARIANCE AND BIAS

1) BR SOLUTION

The perturbation method is utilized in this subsection to analyze the covariance and bias of the proposed BR algorithm. Denoting the solution of (40) is $\widetilde{\boldsymbol{\psi}}'$, thus we have $\widetilde{\boldsymbol{\psi}}'/\widetilde{\psi}'(5) = [\boldsymbol{\psi}'^T, 1]^T$, $\widetilde{\psi}'(5)$ is the last element of $\widetilde{\boldsymbol{\psi}}'$. The equation error at this solution is

$$\begin{aligned}\widetilde{\mathbf{G}}\widetilde{\boldsymbol{\psi}}' &= [-\mathbf{G}, \mathbf{h}] \begin{bmatrix} \boldsymbol{\psi}' \\ 1 \end{bmatrix} \\ &= -\mathbf{G}^o \boldsymbol{\psi}' - \Delta\mathbf{G}\boldsymbol{\psi}' + \mathbf{h}, \end{aligned} \quad (53)$$

where

$$\mathbf{G}_1 = \mathbf{G}_1^o + \Delta\mathbf{G}_1 \quad (54)$$

has been used. Let

$$\check{\mathbf{G}} = [-\mathbf{G}^o, -\Delta\mathbf{G}\boldsymbol{\psi}' + \mathbf{h}], \quad (55)$$

then

$$\widetilde{\mathbf{G}}\widetilde{\boldsymbol{\psi}}' = \check{\mathbf{G}}\widetilde{\boldsymbol{\psi}}'. \quad (56)$$

Following the similar steps from (36) to (40), we shall solve the problem

$$\min_{\boldsymbol{\psi}} \widetilde{\boldsymbol{\psi}}'^T \check{\mathbf{G}}^T \mathbf{W} \check{\mathbf{G}} \widetilde{\boldsymbol{\psi}}' \quad (57a)$$

$$\text{s.t. } \widetilde{\boldsymbol{\psi}}'^T \check{\boldsymbol{\Omega}} \widetilde{\boldsymbol{\psi}}' = const., \quad (57b)$$

where

$$\check{\boldsymbol{\Omega}} = E[\Delta\check{\mathbf{G}}^T \mathbf{W} \Delta\check{\mathbf{G}}], \quad (58)$$

and

$$\check{\mathbf{G}} = \mathbf{G}^o + \Delta\check{\mathbf{G}} \quad (59)$$

has been applied. So the noise of $\check{\mathbf{G}}$ is, after comparing with (55),

$$\Delta\check{\mathbf{G}} = \left[\mathbf{O}_{(2K)\times 4}, -\Delta\mathbf{G}\boldsymbol{\psi}' + \Delta\mathbf{h}\right]. \quad (60)$$

The expression of $\check{\boldsymbol{\Omega}}$ is

$$\check{\boldsymbol{\Omega}} = \begin{bmatrix} \mathbf{O}_{(N+1)\times(N+1)} & \mathbf{0}_{(N+1)} \\ \mathbf{0}_{(N+1)}^T & \check{\Omega} \end{bmatrix}, \quad (61)$$

where $\check{\Omega}$ is a scaler whose value is not important for the following derivation. Differentiating the Lagrangian of (57) and equaling it to zero yield

$$(\check{\mathbf{G}}^T \mathbf{W} \check{\mathbf{G}}) \widetilde{\boldsymbol{\psi}}' = \lambda \check{\boldsymbol{\Omega}} \widetilde{\boldsymbol{\psi}}'. \quad (62)$$

$\check{\mathbf{G}}^T \mathbf{W} \check{\mathbf{G}}$ can be expressed as a block matrix

$$\check{\mathbf{G}}^T \mathbf{W} \check{\mathbf{G}} = \begin{bmatrix} \boldsymbol{\Gamma}_1 & \boldsymbol{\Gamma}_2 \\ \boldsymbol{\Gamma}_2^T & \Gamma_3 \end{bmatrix}, \quad (63)$$

where

$$\begin{aligned} \boldsymbol{\Gamma}_1 &= \mathbf{G}^{oT} \mathbf{W} \mathbf{G}^o \in \mathbb{R}^{4\times 4}, \\ \boldsymbol{\Gamma}_2 &= \mathbf{G}^{oT} \mathbf{W} \mathbf{p} \in \mathbb{R}^{4\times 1}, \\ \Gamma_3 &= \mathbf{p}^T \mathbf{W} \mathbf{p} \in \mathbb{R}. \end{aligned} \quad (64)$$

and

$$\mathbf{p} = -\Delta\mathbf{G}\boldsymbol{\psi}' + \mathbf{h}. \quad (65)$$

Putting (63) back to (62) and considering only the first 4 rows,

$$\left[\mathbf{G}^{oT} \mathbf{W} \mathbf{G}^o, \ -\mathbf{G}^{oT} \mathbf{W} \mathbf{p}\right] \widetilde{\boldsymbol{\psi}}' = \mathbf{0}_4. \quad (66)$$

Dividing both sides by the last element of $\widetilde{\boldsymbol{\psi}}'$ and using $\widetilde{\boldsymbol{\psi}}'/\widetilde{\psi}'(5) = [\boldsymbol{\psi}'^T, 1]^T$ yield

$$\mathbf{G}^{oT} \mathbf{W} \mathbf{G}^o \boldsymbol{\psi}' = \mathbf{G}^{oT} \mathbf{W} \mathbf{p}. \quad (67)$$

Since $\mathbf{h} = \mathbf{h}^o + \Delta\mathbf{h}$ and $\mathbf{h}^o = \mathbf{G}^o \boldsymbol{\psi}^o$, substituting $\boldsymbol{\psi}' = \boldsymbol{\psi}^o + \Delta\boldsymbol{\psi}'$ and (65) to (67) results

$$(\mathbf{G}^{oT} \mathbf{W} \mathbf{G}^o + \mathbf{G}^{oT} \mathbf{W} \Delta\mathbf{G}) \Delta\boldsymbol{\psi}'_1 = -\mathbf{G}^{oT} \mathbf{W} (\Delta\mathbf{G}\boldsymbol{\psi}^o - \Delta\mathbf{h}). \quad (68)$$

Denote

$$\begin{aligned} \mathbf{H}_1 &= \mathbf{G}^{oT} \mathbf{W} \mathbf{G}^o, \\ \mathbf{H}_2 &= (\mathbf{G}^{oT} \mathbf{W} \mathbf{G}^o)^{-1} \mathbf{G}^{oT} \mathbf{W}. \end{aligned} \quad (69)$$

Under the small noise conditions, we have the Neumann approximation [36]

$$\begin{aligned}(\mathbf{H}_1 + \mathbf{G}^{oT} \mathbf{W} \Delta\mathbf{G})^{-1} &= (\mathbf{I} + \mathbf{H}_2 \Delta\mathbf{G})^{-1} \mathbf{H}_1^{-1} \\ &\simeq (\mathbf{I} - \mathbf{H}_2 \Delta\mathbf{G}) \mathbf{H}_1^{-1}. \end{aligned} \quad (70)$$

Putting (70) to (68), the error vector of the solution is

$$\Delta\boldsymbol{\psi}' = -(\mathbf{I} - \mathbf{H}_2 \Delta\mathbf{G}) \mathbf{H}_2 \mathbf{B} \Delta\boldsymbol{\gamma}, \quad (71)$$

where $\Delta\mathbf{G}\boldsymbol{\psi}^o - \Delta\mathbf{h} = \Delta\boldsymbol{\gamma}$ has been used.

The bias is given by the expectation of (71)

$$E[\Delta\boldsymbol{\psi}'] \approx \mathbf{H}_2 E[\Delta\mathbf{G}\mathbf{H}_2 \mathbf{B} \Delta\boldsymbol{\gamma}]. \quad (72)$$

The expectation at the right side is

$$E[\Delta\mathbf{G}\mathbf{H}_2 \mathbf{B} \Delta\boldsymbol{\gamma}] = [\mathbf{q}_1^T, \mathbf{q}_2^T]^T, \quad (73)$$

where $\mathbf{q}_1$ and $\mathbf{q}_2$ are column vectors formed by the diagonal elements of

$$\begin{aligned} \mathbf{Q}_1 &= \mathbf{H}_3(:, 1:K) \mathbf{Q}_a, \\ \mathbf{Q}_2 &= \mathbf{H}_4(:, 1:K) \mathbf{Q}_a, \end{aligned} \quad (74)$$

respectively, and

$$\begin{aligned} \mathbf{H}_3 &= \mathbf{P}_1 \mathbf{H}_2 \mathbf{B}, \\ \mathbf{H}_4 &= \mathbf{P}_2 \mathbf{H}_2 \mathbf{B}. \end{aligned} \quad (75)$$

$\mathbf{P}_1$ and $\mathbf{P}_2$ are given by (92a) and (92b).

The covariance is

$$E[\Delta\boldsymbol{\psi}' \Delta\boldsymbol{\psi}'^T] \approx \mathbf{H}_2 \mathbf{B} \mathbf{Q} \mathbf{B}^T \mathbf{H}_2^T = (\mathbf{G}^{oT} \mathbf{W} \mathbf{G}^o)^{-1}, \quad (76)$$

where the noise terms higher than second order are neglected.

Appendix B proves that the theoretical covariance (76) is equal to the CRLB given by (47) to (51) in Section IV-A under the small noise conditions where

$$\begin{aligned} \theta_k/\Delta\theta_k &\approx 0, \\ f_k/\Delta f_k &\approx 0. \end{aligned} \tag{77}$$

2) MLE

The bias and covariance of a column vector estimation from minimizing a cost function is summarized in [37]. We follow this work to evaluate the performance of the proposed MLE.

The estimate of $\boldsymbol{\psi}$ implies

$$\mathbf{0} = \left.\frac{\partial \mathcal{J}_{ML}}{\partial \boldsymbol{\psi}}\right|_{\boldsymbol{\psi}=\hat{\boldsymbol{\psi}}}, \tag{78}$$

where $\hat{\boldsymbol{\psi}}$ is the estimated value. Taking Taylor series expansion of the right side yields

$$\mathbf{0} \approx \left.\frac{\partial \mathcal{J}_{ML}}{\partial \boldsymbol{\psi}}\right|_{\boldsymbol{\psi}=\boldsymbol{\psi}^o} + \left.\frac{\partial^2 \mathcal{J}_{ML}}{\partial \boldsymbol{\psi}\partial \boldsymbol{\psi}^T}\right|_{\boldsymbol{\psi}=\boldsymbol{\psi}^o} (\hat{\boldsymbol{\psi}} - \boldsymbol{\psi}^o), \tag{79}$$

where $\hat{\boldsymbol{\gamma}}$ is the angle and Doppler corresponding to the estimation $\hat{\boldsymbol{\psi}}$. The gradient vector and Hessian matrix evaluated at the true value are

$$\begin{aligned} \bigtriangledown \mathcal{J}_{ML} &= \left.\frac{\partial \mathcal{J}_{ML}}{\partial \boldsymbol{\psi}}\right|_{\boldsymbol{\psi}=\boldsymbol{\psi}^o} \\ &= 2\left(\frac{\partial \boldsymbol{\gamma}^o}{\partial \boldsymbol{\psi}^{oT}}\right)^T \mathbf{Q}^{-1}(\boldsymbol{\gamma} - \boldsymbol{\gamma}^o), \end{aligned} \tag{80a}$$

$$\begin{aligned} \mathscr{H}(\mathcal{J}_{ML}) &= \left.\frac{\partial^2 \mathcal{J}_{ML}}{\partial \boldsymbol{\psi}\partial \boldsymbol{\psi}^T}\right|_{\boldsymbol{\psi}=\boldsymbol{\psi}^o} \\ &= 2\left(\frac{\partial^2 \boldsymbol{\gamma}^o}{\partial \boldsymbol{\psi}^o \partial \boldsymbol{\psi}^{oT}}\right)^T \mathbf{Q}^{-1}(\boldsymbol{\gamma} - \boldsymbol{\gamma}^o) \\ &\quad - \left(\frac{\partial \boldsymbol{\gamma}^o}{\partial \boldsymbol{\psi}^{oT}}\right)^T \mathbf{Q}^{-1} \frac{\partial \boldsymbol{\gamma}^o}{\partial \boldsymbol{\psi}^{oT}}. \end{aligned} \tag{80b}$$

Combining (79), (80a) and (80b) gives the bias

$$E(\hat{\boldsymbol{\psi}} - \boldsymbol{\psi}^o) \approx -E[\bigtriangledown \mathcal{J}_{ML}]\{E[\mathscr{H}(\mathcal{J}_{ML})]\}^{-1} = \mathbf{0}_4 \tag{81}$$

and covariance

$$\begin{aligned} &E[(\hat{\boldsymbol{\psi}} - \boldsymbol{\psi}^o)(\hat{\boldsymbol{\psi}} - \boldsymbol{\psi}^o)^T] \\ &\approx \{E[\mathscr{H}(\mathcal{J}_{ML})]\}^{-1} E[\bigtriangledown \mathcal{J}_{ML} \overset{T}{\bigtriangledown} \mathcal{J}_{ML}]\{E[\mathscr{H}(\mathcal{J}_{ML})]\}^{-1}, \end{aligned} \tag{82}$$

where the right side of (82) is the CRLB. Therefore,

$$E[(\hat{\boldsymbol{\psi}} - \boldsymbol{\psi}^o)(\hat{\boldsymbol{\psi}} - \boldsymbol{\psi}^o)^T] \approx \mathbf{CRLB}(\boldsymbol{\psi}^o) \tag{83}$$

holds when the small noise conditions (77) are satisfied.

V. ACCELERATION SITUATION

In the previous sections, we have discussed the situation that the velocity is constant. We shall extend the proposed methods to a more complex case that the velocity is uneven and the motion direction is changing in this section.

Let's represent the acceleration as $\boldsymbol{\alpha}$. The position and velocity at the k-th observation are

$$\mathbf{p}_k^o = \mathbf{p}^o + t_k \mathbf{v}^o + \frac{1}{2} t_k^2 \boldsymbol{\alpha}, \tag{84a}$$

$$\mathbf{v}_k^o = \mathbf{v}^o + t_k \boldsymbol{\alpha}. \tag{84b}$$

Substituting (84a) and (84b) to (10) and (15) and following the steps from (16) to (20), we obtain similar expressions as in (21a) and (21b), where

$$\begin{aligned} b_k &= \bar{\mathbf{p}}_k^{oT}(\mathbf{q} - \mathbf{p}^o - t_k \mathbf{v}^o - \frac{1}{2} t_k^2 \boldsymbol{\alpha}), \\ c_k &= -\mathbf{u}_k^{oT}(\mathbf{v}^o + t_k \boldsymbol{\alpha}). \end{aligned} \tag{85}$$

Stacking the equations into a matrix form, we reach (23), where $\mathbf{h}$ is given by (24) where

$$\mathbf{h}_1 = [\mathbf{u}_1, \cdots, \mathbf{u}_K]^T(\mathbf{q} - \frac{1}{2} t_k^2 \boldsymbol{\alpha}), \tag{86a}$$

$$\mathbf{h}_2 = \lambda \mathbf{f} + [t_1 \bar{\mathbf{p}}_1, \cdots, t_K \bar{\mathbf{p}}_K]^T \boldsymbol{\alpha}. \tag{86b}$$

The WTLS method is the same as Section III-A. Some slight changes will make the BR and MLE suitable for use to this case:

(i) For the BR solution, the matrix $\boldsymbol{\Omega}$ is related to the acceleration. In terms of the changes of $\mathbf{h}$, $\mathbf{P}_3$ in (94) shall be

$$\mathbf{P}_3 = \mathrm{diag}\{[\bar{\mathbf{p}}_1^{oT}(\mathbf{q} - \frac{1}{2} t_1^2 \boldsymbol{\alpha}), \cdots, \bar{\mathbf{p}}_K^{oT}(\mathbf{q} - \frac{1}{2} t_K^2 \boldsymbol{\alpha})]\}. \tag{87}$$

The rest of steps are the same as Section III-B presented.

(ii) For the MLE, incorporating acceleration leads to different $\mathbf{K}^i$ in (46). Replacing the $\mathbf{v}^o$ on the right side by $\mathbf{v}_k^o$,

$$\begin{aligned} \frac{\partial f_k^o}{\partial \mathbf{p}^o} &= \frac{\mathbf{v}_k^o}{r_k^o} - \frac{(\mathbf{p}_k^o - \mathbf{q})^T \mathbf{v}_k^o (\mathbf{p}_k^o - \mathbf{q})}{r_k^{o3}}, \\ \frac{\partial f_k^o}{\partial \mathbf{v}^o} &= \frac{(\mathbf{p}_k^o - \mathbf{q}) + t_k \mathbf{v}_k^o}{r_k^o} - \frac{t_k (\mathbf{p}_k^o - \mathbf{q}) \mathbf{v}_k^o (\mathbf{p}_k^o - \mathbf{q})}{r_k^{o3}}. \end{aligned} \tag{88}$$

We shall clarify the performance analysis for this situation. Using (88) instead of (52), we obtain the CRLB for non-constant velocity source. The covariance and bias derivation is still applicable, after the changes in solutions are made.

VI. SIMULATIONS

Numerical simulations have been performed to evaluate the performance of the proposed method. The results are displayed in terms of the RMSE and bias. The WTLS based method, the bias reduction solution and the MLE are represented by WTLS, BR and MLE respectively. The number of ensemble runs is 1000. Without loss of generality, the coordinate origin is set at the observation station. The time interval between two adjacent observations is chosen randomly from the uniform distribution on (0, 2). The receiving antenna is a

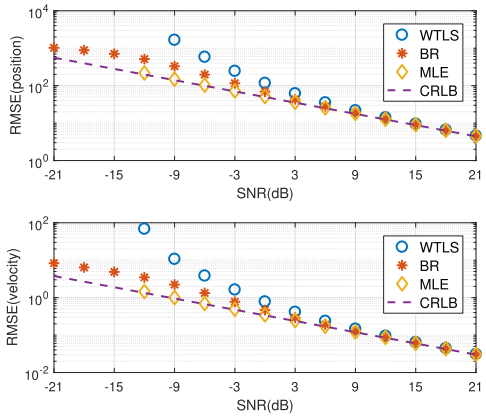

FIGURE 2. RMSE performance as the SNR increases.

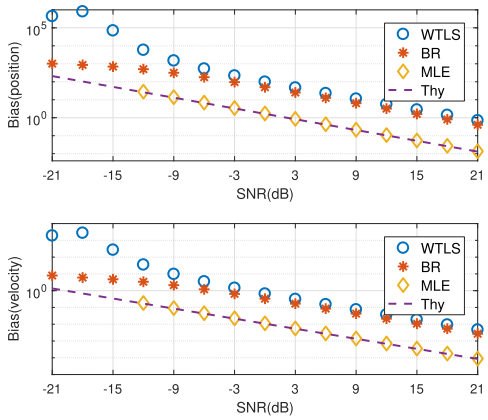

FIGURE 3. Bias performance as the SNR increases.

uniform linear array (ULA) with $M = 16$ elements, where the internal mated spacing is a half-wavelength. The initial position of the source is set at 112 deg with range $R = 1000$ m, which is traveling forward to 73 deg with speed $v = 15$ m/s. That means the transmitter is moving forward from initial position $\mathbf{p} = (-374.6, 927.2)^T$ m with $\mathbf{v} = (4.39, 14.34)^T$ m/s. The emitted frequency is $f = 2.4$ GHz, where the sampling frequency is $f_s = 10$ kHz that satisfies the bandwidth sampling theorem. To show the best performance of WTLS, the covariances of AOA and Doppler estimated at the first step are set as their CRLB given by Appendix C. Since velocity and position are unknown, the proposed methods will present the estimation of location and velocity jointly.

A. CONSTANT VELOCITY

The transmitter location determination is based on 32 frames of the signal ($K = 32$), and each frame includes 64 samples ($N = 64$). The observing time is $T_s = 6.4$ ms for each frame, which is sufficiently short that we can consider the source is temporarily stable. The interval between two adjacent observations is generated randomly with a uniform number generator on the interval (0, 2). The SNR varies from -21 dB to 21 dB. Fig. 2 illustrates the position and velocity estimation performance. The WTLS attends both CRLBs of $\mathbf{p}$ and $\mathbf{v}$ after the SNR increasing to 18 dB. The thresholding effect appears if the SNR is lower than 6 dB. The BR reduces the bias and shows better accuracy than WTLS. Its RMSE achieves CRLB after 9 dB. The MLE is the best and always gives the CRLB performance before diverging. However, like other iterative methods, the result relies on a precious initial solution. The MLE diverges if the SNR lower than -12 dB.

It is shown that the RMSE of WTLS is far away from the corresponding CRLBs in larger noise case from the figures above. To figure out the reason, we plot the biases of $\mathbf{p}$ and $\mathbf{v}$ in Fig. 3. These results verify the reason of deviating CRLB that the bias becomes very large and dominates the RMSE when the SNR is low. BR reduces the bias efficiently so the RMSE is much lower than WTLS especially at low SNR case. MLE has bias much less than that of these two

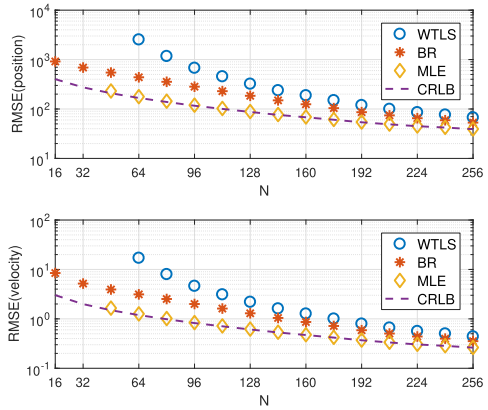

FIGURE 4. RMSE performance as the snapshots increases.

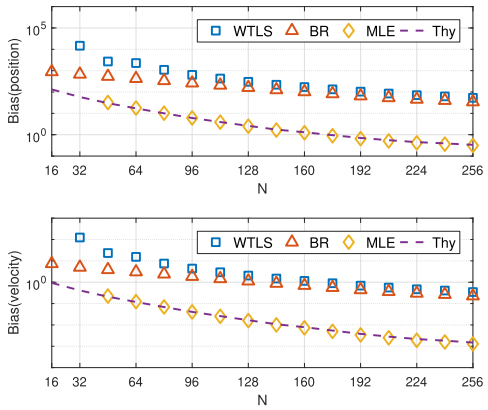

FIGURE 5. Bias performance as the snapshots increases.

closed-form methods but faces the possible divergence problem. And the simulation results match the theory well.

Fig. 4 illustrates the performance as the snapshot increases. SNR is fixed at -9 dB. Others are set as above. It verifies that MLE remains to reach the CRLB performance when the N is above 48. BR is better than WTLS since it reduces the bias as shown in Fig. 5. Also, insufficient snapshots result to a large bias in WTLS and its RMSE diverges. The MLE validates its advancement on both RMSE and bias.

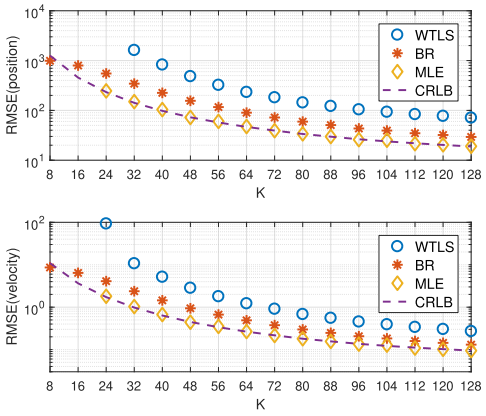

FIGURE 6. RMSE performance as the observation frame increases.

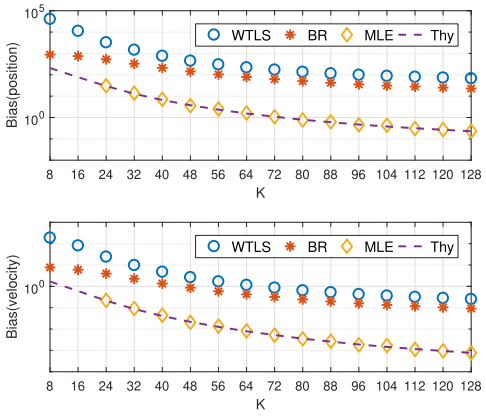

FIGURE 7. Bias performance as the observation frame increases.

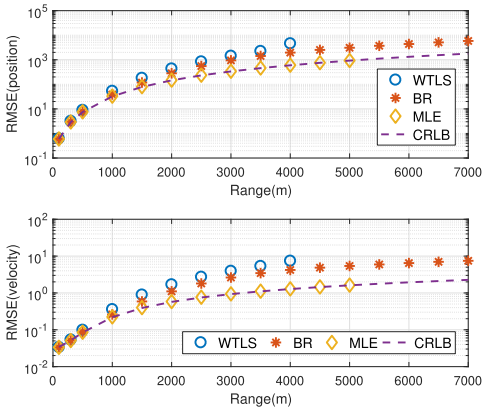

FIGURE 8. RMSE performance as the source range varies.

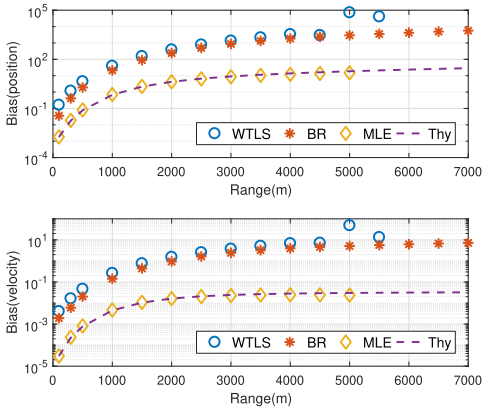

FIGURE 9. Bias performance as the source range varies.

To clarify the relationship with observation frames that determine the equivalent aperture, we fix $N = 64$ and SNR $= -9$ dB. In this example, each observation frame is equal-interval, namely $t_k = (k-1)t_0$ where $t_0 = 1$ is the interval. Other parameters are the same as Fig. 2. It is demonstrated in Fig. 6 that the performance is improved as K is varied over [8, 128]. The WTLS diverges when $K < 32$ because of the large bias. The BR reduces this bias as we expect so its accuracy is better than WTLS. However, both of them do not achieve CRLB. The MLE realizes CRLB performance after $K \geqslant 24$, albeit the non-robustness when K is less. The biases are given in Fig. 7. Again, MLE outperforms the others and match the analytical result.

For more detailed performance evaluations of the proposed methods. we apply the same configuration as before but with different ranges and speeds, where $K = 32$, $N = 64$ and t_k is set as Fig. 2 and Fig. 3.

Fig. 8 and Fig. 9 are the results as the source range varies, where the speed is fixed at 15 m/s. Both the RMSE and bias for all methods increase as the source range increases. The WTLS diverges when the range is large than 4000 m, while the MLE is able to attend the CRLB accuracy until 5000 m. Although the BR solution can't reach the CRLB after 1000 m, it doesn't suffer the divergence problem as the range increased to 7000 m. The estimation bias as the source range increases is illustrated in Fig. 9, with the theoretical bias derived in Section IV included. The MLE gives the theoretical performance and has the smallest bias before divergence occurs. The bias of WTLS increases rapidly when the range is larger than 4500 m. The BR method has bias much larger than the MLE, but it is more robust.

Fig. 10 and Fig. 11 demonstrate the estimation performance by fixing the source range at 1000 m while increasing the speed. Again, the MLE behaves the best for both RMSE and bias as expected. However, it diverges if the speed is not sufficiently fast, such as lower than 6 m/s in this simulation. The WTLS is the worst, and its RMSE becomes very significant due to the large bias if the speed is less than 6 m/s. The BR method is stable as the speed varies, and it almost reaches the CRLB if the speed is larger than 18 m/s. But its bias is much larger than the MLE. These results are not unexpected because faster source gives a larger equivalent aperture if the observation time is the same.

B. NOISY VELOCITY

The velocity cannot be maintained as constant in practice. In such a case the proposed solution provides the mean of the actual velocity over the observation period. Assume that the

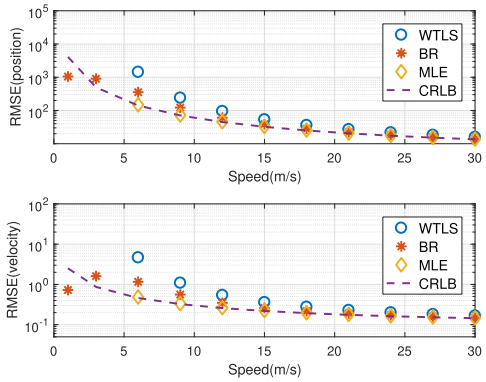

FIGURE 10. RMSE performance as the source speed varies.

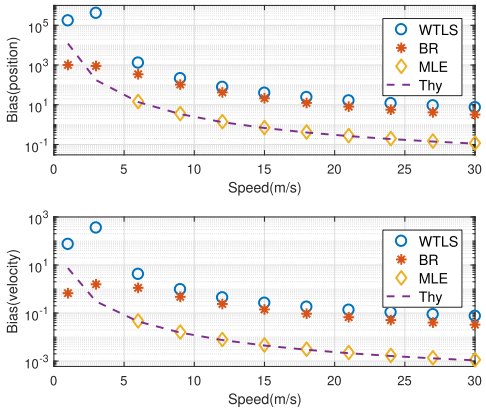

FIGURE 11. Bias performance as the source speed varies.

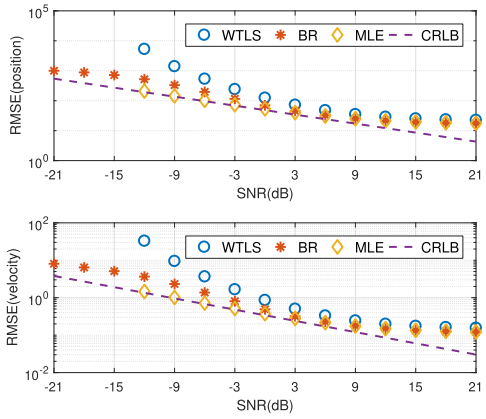

FIGURE 12. RMSE vs. SNR when the velocity is noisy.

actual velocity at different time instance k varies with respect to the mean value $\mathbf{v}^o$,

$$\mathbf{v}_k^o = \mathbf{v}^o + \boldsymbol{\epsilon}, \tag{89}$$

where $\boldsymbol{\epsilon}$ is Gaussian random noise with zero mean and covariance $\sigma_v^2\mathbf{I}$. Fig. 12 and Fig. 13 show the estimation performance of the position and mean velocity value where $\sigma_v^2 = 0.1$ (m/s)^2. The other parameters are set the same as Fig. 2 and Fig. 3. The MLE provides CRLB performance when the

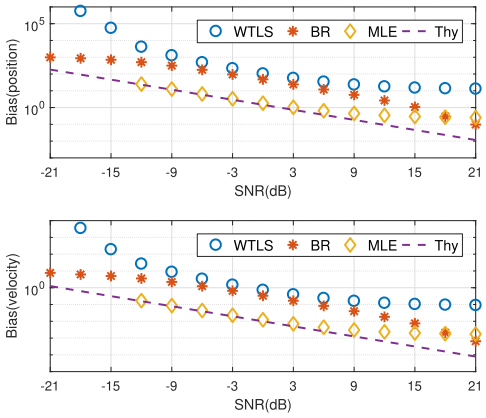

FIGURE 13. Bias vs. SNR when the velocity is noisy.

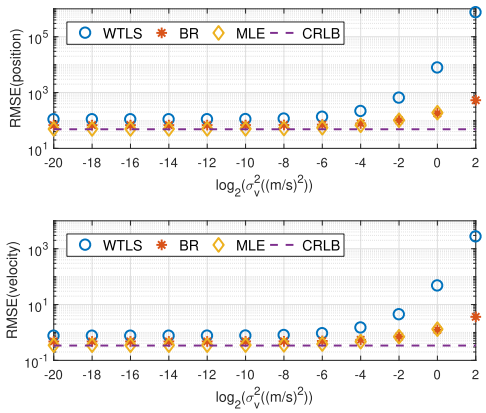

FIGURE 14. RMSE vs. velocity noise power (SNR = 0 dB).

SNR is lower than 6 dB before it diverges. After the SNR increases above 6 dB, the model error is significant, where all three methods reach constant RMSE of the estimates since the non-constant velocity distorts the results. As we expect, the MLE has the smallest bias, while the BR lower the bias than WTLS. It is interesting that the bias of BR is lower than MLE when the SNR = 21 dB.

Fig. 14 and Fig. 15 illustrate the performance when the SNR is fixed at 0 dB. The velocity noise power varies from 2^{-20} (m/s)^2 to 4 (m/s)^2. The other parameters are set as above. The MLE keeps the best RMSE and bias for both position and velocity estimates. The performance deviates from the CRLB if $\sigma_v^2 > 2^{-6}$ (m/s)^2, and it diverges after the noise increases over 1 (m/s)^2. The BR solution is better than that of WTLS. It performs similarly with to MLE after $\sigma_v^2 > 2^{-4}$ (m/s)^2. Again, the proposed BR and MLE methods provide CRLB accuracy if the velocity noise is small.

C. ACCELERATED MOTION

Next we shall verify the performance while the velocity is uneven and changing direction, where the acceleration is constant. The initial speed is $v = 8$ m/s, where the original moving direction is 73 deg as above. For simplicity,

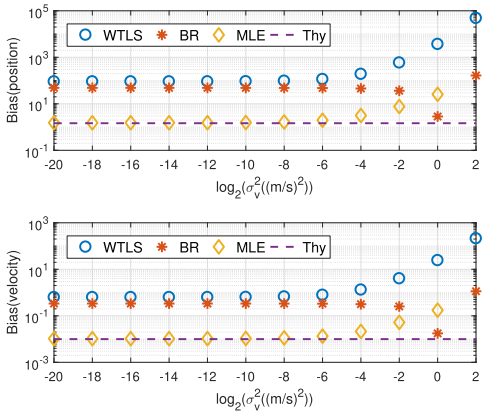

FIGURE 15. Bias vs. velocity noise power (SNR = 0 dB).

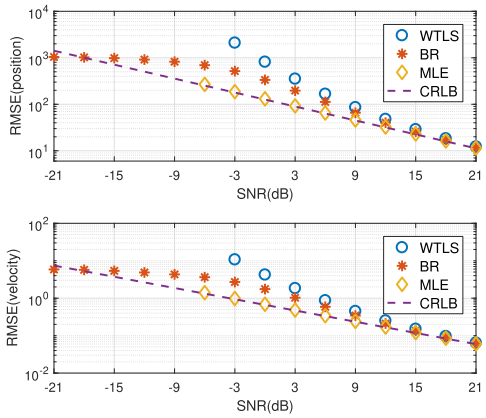

FIGURE 16. RMSE performance while the velocity is uneven and changing direction.

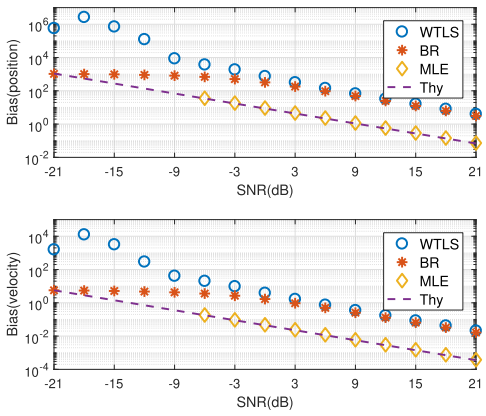

FIGURE 17. Bias performance while the velocity is uneven and changing direction.

the acceleration is known $\boldsymbol{\alpha} = [0.2034, -0.4568]^T$. The other parameters are set as Fig. 2 and Fig. 3. Noting that $\mathbf{v}$ and $\boldsymbol{\alpha}$ are not on the same straight line, both $\|\mathbf{v}_k^o\|$ and $\arctan(v_k^o(2)/v_k^o(1))$ varies.

Fig. 16 and Fig. 17 present the RMSE and bias result while the SNR increases. The plots are similar to Fig. 2 and Fig. 3. The proposed MLE reaches the CRLB accuracy when the SNR is above -6 dB, and the bias matches the theory well. It outperforms both WTLS and BR before the iteration diverges. The BR estimator has no divergence problem, which has lower bias and approaches the CRLB better than WTLS.

VII. CONCLUSION

This paper has proposed three single station localization methods for moving transmitter. The thinking of inverse synthesis aperture is utilized to increase the equivalent aperture, which realizes the single station localization and improves the accuracy. We illustrate the method based on WTLS results large bias first so that a bias reduction method has been developed. This BR solution attends CRLB under the small noise condition. Then the Gauss-Newton iteration method resulting of MLE is implied to improve the accuracy further. This MLE shows its advantages in both RMSE and bias. Simulations validate the expected performance. One of the limitations is that this two-steps method ignore the constraint that all measurements are correlative, which distorts the performance. The further study may manage to handle this problem. The challenging scenario is uneven velocity and changing the direction of motion. In such a situation, the proposed methods can only give the average velocity and requires the detection of motion changes. Three methods are applicable for accelerated motion after some changes if the acceleration is known. A better problem formulation that takes such a scenario into account may provide better results. This is a subject for further study.

APPENDIX A
EXPRESSION OF (41)

Substituting (37) to (41),

$$\boldsymbol{\Omega} = E\begin{bmatrix} \Delta\mathbf{G}^T\mathbf{W}\Delta\mathbf{G} & -\Delta\mathbf{G}^T\mathbf{W}\Delta\mathbf{h} \\ -\Delta\mathbf{h}^T\mathbf{W}\Delta\mathbf{G} & \Delta\mathbf{h}^T\mathbf{W}\Delta\mathbf{h} \end{bmatrix}. \tag{90}$$

The expressions of $\Delta\mathbf{G}$ and $\Delta\mathbf{h}$ are given by, after putting (17)-(18) to (24) and (26),

$$\begin{aligned} \Delta\mathbf{G} &= [\Delta\mathbf{G}_1^T, \Delta\mathbf{G}_2^T]^T, \\ \Delta\mathbf{G}_1 &= \Delta\boldsymbol{\Theta}\mathbf{P}_1, \\ \Delta\mathbf{G}_2 &= \Delta\boldsymbol{\Theta}\mathbf{P}_2, \end{aligned} \tag{91}$$

where

$$\mathbf{P}_1 = \begin{bmatrix} \bar{\mathbf{p}}_1^{oT} & t_1\bar{\mathbf{p}}_1^{oT} \\ \vdots & \vdots \\ \bar{\mathbf{p}}_K^{oT} & t_K\bar{\mathbf{p}}_K^{oT} \end{bmatrix}, \tag{92a}$$

$$\mathbf{P}_2 = \begin{bmatrix} \mathbf{0}^T & \mathbf{u}_1^{oT} \\ \vdots & \vdots \\ \mathbf{0}^T & \mathbf{u}_K^{oT} \end{bmatrix}, \tag{92b}$$

$$\Delta\boldsymbol{\Theta} = \mathrm{diag}\{\Delta\boldsymbol{\theta}\}. \tag{92c}$$

and

$$\Delta\mathbf{h} = [\Delta\mathbf{h}_1^T, \Delta\mathbf{h}_2^T]^T,$$

$$\begin{aligned}\Delta\mathbf{h}_1 &= \mathbf{P}_3\Delta\boldsymbol{\theta},\\ \Delta\mathbf{h}_2 &= \lambda\Delta\mathbf{f},\end{aligned} \tag{93}$$

where

$$\mathbf{P}_3 = \text{diag}\{[\bar{\mathbf{p}}_1^o,\cdots,\bar{\mathbf{p}}_K^o]^T\mathbf{q}\}. \tag{94}$$

Let us partition $\mathbf{W}$ to block matrix

$$\mathbf{W} = \begin{bmatrix}\mathbf{W}_1 & \mathbf{W}_2\\ \mathbf{W}_3 & \mathbf{W}_4\end{bmatrix}, \tag{95}$$

each block is $K\times K$. Applying (95) to each block of $\boldsymbol{\Omega}$,

$$\begin{aligned}E[\Delta\mathbf{G}^T\mathbf{W}\Delta\mathbf{G}] &= E[\Delta\mathbf{G}_1^T\mathbf{W}_1\Delta\mathbf{G}_1] + E[\Delta\mathbf{G}_1^T\mathbf{W}_2\Delta\mathbf{G}_2]\\ &\quad + E[\Delta\mathbf{G}_2^T\mathbf{W}_3\Delta\mathbf{G}_1] + E[\Delta\mathbf{G}_2^T\mathbf{W}_4\Delta\mathbf{G}_2],\end{aligned} \tag{96a}$$

$$E[\Delta\mathbf{G}^T\mathbf{W}\Delta\mathbf{h}] = E[\Delta\mathbf{G}_1^T\mathbf{W}_1\Delta\mathbf{h}_1] + E[\Delta\mathbf{G}_2^T\mathbf{W}_3\Delta\mathbf{h}_1], \tag{96b}$$

$$E[\Delta\mathbf{h}^T\mathbf{W}\Delta\mathbf{h}] = E[\Delta\mathbf{h}_1^T\mathbf{W}_1\Delta\mathbf{h}_1] + E[\Delta\mathbf{h}_2^T\mathbf{W}_4\Delta\mathbf{h}_2]. \tag{96c}$$

where $E[\Delta\mathbf{G}_1^T\mathbf{W}_2\Delta\mathbf{h}_2]$, $E[\Delta\mathbf{G}_2^T\mathbf{W}_4\Delta\mathbf{h}_2]$, $E[\Delta\mathbf{h}_1^T\mathbf{W}_2\Delta\mathbf{h}_1]$ and $E[\Delta\mathbf{h}_2^T\mathbf{W}_3\Delta\mathbf{h}_1]$ are ignored since they are zeros according to (91) and (93) under the assumption that angle and Doppler measurements are approximately independent.

Substituting (91) and (93) to (96a), (96b) and (96c) yields

$$\begin{aligned}E[\Delta\mathbf{G}^T\mathbf{W}\Delta\mathbf{G}] &= \mathbf{P}_1^T(\mathbf{Q}_a\odot\mathbf{W}_1)\mathbf{P}_1 + \mathbf{P}_1^T(\mathbf{Q}_a\odot\mathbf{W}_2)\mathbf{P}_2\\ &\quad + \mathbf{P}_2^T(\mathbf{Q}_a\odot\mathbf{W}_3)\mathbf{P}_1 + \mathbf{P}_2^T(\mathbf{Q}_a\odot\mathbf{W}_4)\mathbf{P}_2,\end{aligned} \tag{97a}$$

$$\begin{aligned}E[\Delta\mathbf{G}^T\mathbf{W}\Delta\mathbf{h}] &= [\mathbf{P}_1^T(\mathbf{Q}_a\odot(\mathbf{W}_1\mathbf{P}_3))\\ &\quad + \mathbf{P}_2^T(\mathbf{Q}_a\odot(\mathbf{W}_3\mathbf{P}_3))]\cdot\mathbf{1}_K,\end{aligned} \tag{97b}$$

$$E[\Delta\mathbf{h}^T\mathbf{W}\Delta\mathbf{h}] = \text{tr}(\mathbf{P}_3^T\mathbf{W}_1\mathbf{P}_3\mathbf{Q}_a) + \lambda^2\,\text{tr}(\mathbf{W}_4\mathbf{Q}_f). \tag{97c}$$

APPENDIX B
COMPARING WITH CRLB

Substituting (31) to (76) and taking inverse yield

$$\mathbf{G}^{oT}\mathbf{W}\mathbf{G}^o = \mathbf{G}^{oT}\mathbf{B}^{-T}\mathbf{Q}^{-1}\mathbf{B}^{-1}\mathbf{G}^o. \tag{98}$$

Using (26), (28) and the block matrix inversion, we obtain

$$\mathbf{B}^{-1}\mathbf{G}^o = \begin{bmatrix}\mathbf{B}_1^{-1}\mathbf{G}_1^o\\ -\mathbf{B}_3^{-1}\mathbf{B}_2\mathbf{B}_1^{-1}\mathbf{G}_1^o + \mathbf{B}_3^{-1}\mathbf{G}_2^o\end{bmatrix}. \tag{99}$$

Denoting $[\{\bullet\}](k,:)$ is the k-th row of matrix $\{\bullet\}$, $k = 1,2,\cdots,K$. Putting (27a) and (29a) to $\mathbf{B}_1^{-1}\mathbf{G}_1^o$, the expression of the k-th row is

$$[\mathbf{B}_1^{-1}\mathbf{G}_1^o](k,:) = \begin{bmatrix}\dfrac{\mathbf{u}_k^{oT}}{b_k}, & \dfrac{t_k\mathbf{u}_k^{oT}}{b_k}\end{bmatrix}. \tag{100}$$

Noting $b_k = -r_k^o$ with the true value of AOAs, and

$$\mathbf{u}_k^o = \begin{bmatrix}\sin\theta_k^o\\ -\cos\theta_k^o\end{bmatrix} = \frac{1}{r_k^o}\begin{bmatrix}y^o + t_k v_y^o - y_s\\ -x^o + t_k v_x^o - x_s\end{bmatrix}, \tag{101}$$

it is conclude that

$$[\mathbf{B}_1^{-1}\mathbf{G}_1^o](k,:) = \frac{\partial\theta_k^o}{\partial\boldsymbol{\psi}^o}. \tag{102}$$

Similarly,

$$\begin{aligned}&[-\mathbf{B}_3^{-1}\mathbf{B}_2\mathbf{B}_1^{-1}\mathbf{G}_1^o + \mathbf{B}_3^{-1}\mathbf{G}_2^o](k,:)\\ &= \frac{\mathbf{u}_k^{oT}\mathbf{v}^o}{\lambda}\begin{bmatrix}\dfrac{\mathbf{u}_k^{oT}}{b_k}, & \dfrac{t_k\mathbf{u}_k^{oT}}{b_k}\end{bmatrix} + \frac{1}{\lambda}\left[\mathbf{0}^T, -\bar{\mathbf{p}}_k^{oT}\right]\\ &= \frac{\mathbf{u}_k^{oT}\mathbf{v}^o}{\lambda}\frac{\partial\theta_k^o}{\partial\boldsymbol{\psi}^o} + \frac{1}{\lambda}\left[\mathbf{0}^T, -\bar{\mathbf{p}}_k^{oT}\right].\end{aligned} \tag{103}$$

Since $\bar{\mathbf{p}}_k^o = [\cos\theta_k^o, \sin\theta_k^o]^T$ is defined as (14), comparing (103) and (51) yields

$$[-\mathbf{B}_3^{-1}\mathbf{B}_2\mathbf{B}_1^{-1}\mathbf{G}_1^o + \mathbf{B}_3^{-1}\mathbf{G}_2^o](k,:) = \frac{\partial f_k^o}{\partial\boldsymbol{\psi}^o}. \tag{104}$$

Hence, according to (102) and (104)

$$\mathbf{B}^{-1}\mathbf{G}^o = \frac{\partial\boldsymbol{\gamma}^o}{\partial\boldsymbol{\psi}^{oT}}. \tag{105}$$

Consequentially, under the small noise conditions (77), comparing (48), (76) and (105) shows that

$$\text{cov}(\boldsymbol{\psi}) \approx \mathbf{CRLB}(\boldsymbol{\psi}^o) \tag{106}$$

holds.

APPENDIX C
CRLB OF AOA AND DOPPLER USING MODEL (6)

The AOA and Doppler frequency are estimated from single observation frame given by (8) independently. For simplicity and convenience, the subscript $_k$ for denoting the k-th frame is dropped bellow,

$$\mathbf{r} = b\bar{\mathbf{A}}\bar{\mathbf{s}} + \boldsymbol{\eta}. \tag{107}$$

$\bar{\mathbf{A}}$ and $\bar{\mathbf{s}}$ are (9b) and (9c) dropping $_k$. The unknowns are denoted by

$$\boldsymbol{\kappa} = [\theta, f, \check{\mathbf{b}}], \tag{108}$$

where $\check{\mathbf{b}} = [\Re\{b\}, \Im\{b\}]$. Under the assumption that noise $\boldsymbol{\eta}$ is independent across time and array elements, whose covariance matrix is $\sigma^2\mathbf{I}_{MN}$, we can find the expression of FIM from [38],

$$\mathbf{FIM}(\boldsymbol{\kappa}^o) = \frac{2}{\sigma^2}\Re\left\{\left(\frac{\partial\mathbf{r}^o}{\partial\boldsymbol{\kappa}^{oT}}\right)^H\frac{\partial\mathbf{r}^o}{\partial\boldsymbol{\kappa}^{oT}}\right\}. \tag{109}$$

Partitioning the FIM to block form,

$$\mathbf{FIM}(\boldsymbol{\kappa}^o) = \begin{bmatrix}F_{\theta\theta} & F_{\theta f} & \mathbf{F}_{\theta\check{\mathbf{b}}}\\ F_{\theta f} & F_{ff} & \mathbf{F}_{f\check{\mathbf{b}}}\\ \mathbf{F}_{\theta\check{\mathbf{b}}}^T & \mathbf{F}_{f\check{\mathbf{b}}}^T & \mathbf{F}_{\check{\mathbf{b}}\check{\mathbf{b}}}\end{bmatrix}, \tag{110}$$

the blocks are given as follow,

$$F_{\theta\theta} = \frac{2}{\sigma^2}\left\|b\mathbf{X}\bar{\mathbf{A}}\bar{\mathbf{s}}\right\|^2, \tag{111a}$$

$$F_{\theta f} = \frac{2\|b\|^2}{\sigma^2}\Re\left\{\bar{\mathbf{s}}^H\bar{\mathbf{A}}^H\mathbf{X}^H\mathbf{Y}\bar{\mathbf{A}}\bar{\mathbf{s}}\right\}, \tag{111b}$$

$$\mathbf{F}_{\theta\check{\mathbf{b}}} = \frac{2}{\sigma^2}\left[\Re\left\{(b\mathbf{X}\bar{\mathbf{A}}\bar{\mathbf{s}})^H\bar{\mathbf{A}}\bar{\mathbf{s}}\right\}, -\Im\left\{(b\mathbf{X}\bar{\mathbf{A}}\bar{\mathbf{s}})^H\bar{\mathbf{A}}\bar{\mathbf{s}}\right\}\right], \tag{111c}$$

$$F_{ff} = \frac{2\|b\|^2}{\sigma^2}\left\|\mathbf{Y}\bar{\mathbf{A}}\bar{\mathbf{s}}\right\|^2, \tag{112a}$$

$$\mathbf{F}_{f\check{\mathbf{b}}} = \frac{2}{\sigma^2}\left[\Re\left\{(b\mathbf{Y}\bar{\mathbf{A}}\bar{\mathbf{s}})^H\bar{\mathbf{A}}\bar{\mathbf{s}}\right\}, -\Im\left\{(b\mathbf{Y}\bar{\mathbf{A}}\bar{\mathbf{s}})^H\bar{\mathbf{A}}\bar{\mathbf{s}}\right\}\right], \tag{112b}$$

$$\mathbf{F}_{\check{\mathbf{b}}\check{\mathbf{b}}} = \frac{2}{\sigma^2}\begin{bmatrix}\bar{\mathbf{s}}^H\bar{\mathbf{A}}^H\bar{\mathbf{A}}\bar{\mathbf{s}} & \mathbf{O}\\ \mathbf{O} & \bar{\mathbf{s}}^H\bar{\mathbf{A}}^H\bar{\mathbf{A}}\bar{\mathbf{s}}\end{bmatrix}, \tag{113}$$

where

$$\mathbf{X} = -\frac{j2\pi\sin\theta}{\lambda}(\mathbf{I}_N\otimes\mathbf{\Lambda}), \tag{114a}$$

$$\mathbf{Y} = \frac{j2\pi}{f_s}(\mathrm{diag}\{0,1,\cdots,N-1\}\otimes\mathbf{I}_M). \tag{114b}$$

ACKNOWLEDGMENT

The authors would like to thank the anonymous reviewers for providing valuable comments and suggestions that have helped improving the quality of the paper. And thanks are due to Dr. K. C. Ho for the constructive suggestions and valuable discussions.

REFERENCES

[1] R. Di Taranto, S. Muppirisetty, R. Raulefs, D. Slock, T. Svensson, and H. Wymeersch, "Location-aware communications for 5G networks: How location information can improve scalability, latency, and robustness of 5G," *IEEE Signal Process. Mag.*, vol. 31, no. 6, pp. 102–112, Nov. 2014.

[2] A. Tahat, G. Kaddoum, S. Yousefi, S. Valaee, and F. Gagnon, "A look at the recent wireless positioning techniques with a focus on algorithms for moving receivers," *IEEE Access*, vol. 4, pp. 6652–6680, 2016.

[3] R. Karlsson and F. Gustafsson, "The future of automotive localization algorithms: Available, reliable, and scalable localization: Anywhere and anytime," *IEEE Signal Process. Mag.*, vol. 34, no. 2, pp. 60–69, Mar. 2017.

[4] O. Bialer, D. Raphaeli, and A. J. Weiss, "Efficient time of arrival estimation algorithm achieving maximum likelihood performance in dense multipath," *IEEE Trans. Signal Process.*, vol. 60, no. 3, pp. 1241–1252, Mar. 2012.

[5] Y. Wang and K. C. Ho, "An asymptotically efficient estimator in closed-form for 3-D AOA localization using a sensor network," *IEEE Trans. Wireless Commun.*, vol. 14, no. 12, pp. 6524–6535, Dec. 2015.

[6] L. Lin, H. C. So, F. K. W. Chan, Y. T. Chan, and K. C. Ho, "A new constrained weighted least squares algorithm for TDOA-based localization," *Signal Process.*, vol. 93, no. 11, pp. 2872–2878, 2013.

[7] Y. Wang and K. C. Ho, "TDOA positioning irrespective of source range," *IEEE Trans. Signal Process.*, vol. 65, no. 6, pp. 1447–1460, Mar. 2017.

[8] Y. Zou, H. Liu, W. Xie, and Q. Wan, "Semidefinite programming methods for alleviating sensor position error in TDOA localization," *IEEE Access*, vol. 5, pp. 23111–23120, 2017.

[9] K. C. Ho and W. Xu, "An accurate algebraic solution for moving source location using TDOA and FDOA measurements," *IEEE Trans. Signal Process.*, vol. 52, no. 9, pp. 2453–2463, Sep. 2004.

[10] K. C. Ho, X. Lu, and L. Kovavisaruch, "Source localization using TDOA and FDOA measurements in the presence of receiver location errors: Analysis and solution," *IEEE Trans. Signal Process.*, vol. 55, no. 2, pp. 684–696, Feb. 2007.

[11] H. Yu, G. Huang, J. Gao, and B. Liu, "An efficient constrained weighted least squares algorithm for moving source location using TDOA and FDOA measurements," *IEEE Trans. Wireless Commun.*, vol. 11, no. 1, pp. 44–47, Jan. 2012.

[12] Y. Wang and Y. Wu, "An efficient semidefinite relaxation algorithm for moving source localization using TDOA and FDOA measurements," *IEEE Commun. Lett.*, vol. 21, no. 1, pp. 80–83, Jan. 2017.

[13] A. Weiss, "Direct geolocation of wideband emitters based on delay and Doppler," *IEEE Trans. Signal Process.*, vol. 59, no. 6, pp. 2513–2521, Jun. 2011.

[14] T. Tirer and A. J. Weiss, "High resolution localization of narrowband radio emitters based on Doppler frequency shifts," *Signal Process.*, vol. 141, pp. 288–298, Dec. 2017.

[15] J. Yin, Q. Wan, S. Yang, and K. C. Ho, "A simple and accurate TDOA-AOA localization method using two stations," *IEEE Signal Process. Lett.*, vol. 23, no. 1, pp. 144–148, Jan. 2016.

[16] Y. Sun, Z.-P. Zhou, S.-L. Tang, X. K. Ding, J. Yin, and Q. Wan, "3D hybrid TOA-AOA source localization using an active and a passive station," in *Proc. IEEE 13th Int. Conf. Signal Process. (ICSP)*, Nov. 2016, pp. 257–260.

[17] T. Jia, H. Wang, X. Shen, Z. Jiang, and K. He, "Target localization based on structured total least squares with hybrid TDOA-AOA measurements," *Signal Process.*, vol. 143, pp. 211–221, Feb. 2018.

[18] H. W. Wei, R. Peng, Q. Wan, Z. X. Chen, and S. F. Ye, "Multidimensional scaling analysis for passive moving target localization with TDOA and FDOA measurements," *IEEE Trans. Signal Process.*, vol. 58, no. 3, pp. 1677–1688, Mar. 2010.

[19] Y. Zhao, Y. Zhao, and C. Zhao, "A novel algebraic solution for moving target localization in multi-transmitter multi-receiver passive radar," *Signal Process.*, vol. 143, pp. 303–310, Feb. 2018.

[20] M. Oispuu and U. Nickel, "Direct detection and position determination of multiple sources with intermittent emission," *Signal Process.*, vol. 90, no. 12, pp. 3056–3064, Dec. 2010.

[21] A. Amar and A. J. Weiss, "Localization of narrowband radio emitters based on Doppler frequency shifts," *IEEE Trans. Signal Process.*, vol. 56, no. 11, pp. 5500–5508, Nov. 2008.

[22] W. M. Brown, "Synthetic aperture radar," *IEEE Trans. Aerosp. Electron. Syst.*, vol. AES-3, no. 2, pp. 217–229, Mar. 1967.

[23] J. C. Curlander and R. N. McDonough, *Synthetic Aperture Radar: Systems and Signal Processing*. New York, NY, USA: Wiley, 1991.

[24] Y. Yang, X. Cong, K. Long, Y. Luo, W. Xie, and Q. Wan, "MRF model-based joint interrupted SAR imaging and coherent change detection via variational Bayesian inference," *Signal Process.*, vol. 151, pp. 144–154, Oct. 2018.

[25] D. R. Wehner, *High Resolution Radar*. Norwood, MA, USA: Artech House, 1987.

[26] P. Stoica and N. Arye, "MUSIC, maximum likelihood, and Cramer-Rao bound," *IEEE Trans. Acoust., Speech, Signal Process.*, vol. 37, no. 5, pp. 720–741, May 1989.

[27] F. Wen, Q. Wan, R. Fan, and H. Wei, "Improved MUSIC algorithm for multiple noncoherent subarrays," *IEEE Signal Process. Lett.*, vol. 21, no. 5, pp. 527–530, May 2014.

[28] W. Xie, F. Wen, J. Liu, and Q. Wan, "Source association, DOA, and fading coefficients estimation for multipath signals," *IEEE Trans. Signal Process.*, vol. 65, no. 11, pp. 2773–2786, Jun. 2017.

[29] F. Sun, Q. Wu, P. Lan, G. Ding, and L. Chen, "Real-valued DOA estimation with unknown number of sources via reweighted nuclear norm minimization," *Signal Process.*, vol. 148, pp. 48–55, Jul. 2018.

[30] R. Bamler, "Doppler frequency estimation and the Cramer-Rao bound," *IEEE Trans. Geosci. Remote Sens.*, vol. 29, no. 3, pp. 385–390, May 1991.

[31] B. Friedlander, "On the Cramer–Rao bound for time delay and Doppler estimation," *IEEE Trans. Inf. Theory*, vol. 30, no. 3, pp. 575–580, May 1984.

[32] S. Chen, F. Xi, and Z. Liu, "A general sequential delay-Doppler estimation scheme for sub-Nyquist pulse-Doppler radar," *Signal Process.*, vol. 135, pp. 210–217, Jun. 2017.

[33] K. C. Ho and Y. T. Chan, "An asymptotically unbiased estimator for bearings-only and Doppler-bearing target motion analysis," *IEEE Trans. Signal Process.*, vol. 54, no. 3, pp. 809–822, Mar. 2006.

[34] K. C. Ho, "Bias reduction for an explicit solution of source localization using TDOA," *IEEE Trans. Signal Process.*, vol. 60, no. 5, pp. 2101–2114, May 2012.

[35] S. M. Kay, *Fundamentals of Statistical Signal Processing: Estimation Theory*, vol. 1. Englewood Cliffs, NJ, USA: Prentice-Hall, 1993.

[36] T. K. Moon and W. C. Stirling, *Mathematical Methods and Algorithms for Signal Processing*. Upper Saddle River, NJ, USA: Prentice-Hall, 2000.

[37] H. C. So, Y. T. Chan, K. C. Ho, and Y. Chen, "Simple formulae for bias and mean square error computation [DSP tips and tricks]," *IEEE Signal Process. Mag.*, vol. 30, no. 4, pp. 162–165, Jul. 2013.

[38] H. L. Van Trees, *Optimum Array Processing: Part IV of Detection, Estimation, and Modulation Theory*. Hoboken, NJ, USA: Wiley, 2004.

YIMAO SUN (S'15) was born in 1990. He received the B.S. degree from the School of Electronic Engineering, University of Electronic Science and Technology of China (UESTC), Chengdu, China, in 2013, where he is currently pursuing the Ph.D. degree in information and communication engineering. From 2017 to 2018, he was awarded a Scholarship under the State Scholarship Fund to pursue his study with the Electrical Engineering and Computer Science Department, University of Missouri, Columbia, MO, USA, as a Joint Ph.D. Student. His research interests include passive localization, direct position determination, array signal processing and time delay estimation.

QUN WAN (M'04) received the B.Sc. degree in electronic engineering from Nanjing University in 1993, and the M.Sc. degree and Ph.D. degrees from the University of Electronic Science and Technology of China (UESTC) in 1996 and 2001 respectively, both in electronic engineering. From 2001 to 2003, he held a post-doctoral position at the Department of Electronic Engineering, Tsinghua University. Since 2004, he has been a Professor with the Department of Electronic Engineering, UESTC. He is currently the Director of the Joint Research Lab of Array Signal Processing and the Associate Dean of the School of Electronic Engineering. His research interests include direction finding, radio localization, and signal processing based on information criterion.